doi.org/10.36721/PJPS.2026.39.8.233.1

Fumaric acid regulates morphine tolerance in bone cancer pain through spinal MrgC receptor modulation

Sijie Liu, Minghao Tang, Jing Zhao, Lulu Zhang and Jidong Lv*
Department of Anesthesiology, Jiashan First People's Hospital, Jiaxing, Zhejiang, China

Abstract: **Background**: Bone cancer pain (BCP) represents a debilitating complication that profoundly impacts patient quality of life and predisposes to psychological comorbidities, including depression and anxiety. **Objectives**: To investigate the effect of fumaric acid on morphine tolerance in BCP via spinal MrgC receptors. **Methods**: This study adopted an *in-vivo* animal experiment design. The BCP mouse model was established and divided into the Vehicle group, the fumaric acid monotherapy group with different doses, the fumaric acid + morphine combination group, the normal saline + morphine control group and the fumaric acid + normal saline control group. Intervention is carried out through intrathecal administration. Pain behavior tests such as the threshold for mechanical foot retraction, the number of spontaneous foot lifts, the duration of foot lift protection and the latency period of cold pain foot retraction were evaluated. The expression level of MrgC protein in spinal cord tissue was detected by Western blotting and immunohistochemistry. **Results**: Fumaric acid dose-dependently attenuated BCP and delayed morphine tolerance, with EC_{50} values of 69.18 mg/kg (mechanical) and 99.78 mg/kg (cold). Its effects correlated with downregulation of spinal MrgC expression. **Conclusion**: Fumaric acid alleviates BCP and delays morphine tolerance by down-regulating the expression of spinal MrgC receptors. MrgC receptors are potential new therapeutic targets.

Keywords: Bone cancer pain; Fumaric acid; Morphine; Spinal MrgC receptor; Tolerance

Submitted on 29-08-2025 – Revised on 28-10-2025 – Accepted on 13-11-2025

INTRODUCTION

Cancer remains the leading cause of global death (Ni *et al*., 2024), among which bone cancer pain (BCP) represents a debilitating complication that profoundly impacts patient quality of life and predisposes to psychological comorbidities, including depression and anxiety (Zhang *et al*., 2024). Opioids like morphine remain first-line analgesics for moderate-to-severe cancer pain, yet prolonged use induces spinal neuroplasticity alterations, μ-opioid receptor (MOR) desensitization, G protein-coupled signaling dysregulation and neuroimmune dysfunctions (Ahmadi *et al*., 2024), but the mechanism is still unclear. Substantial emerging evidence implicates spinal cord-level neural mechanisms as pivotal in BCP pathogenesis. In recent years, researchers have gradually turned their attention to exploring new molecular targets to find more effective treatments to overcome morphine tolerance and alleviate patients' symptoms.

Fumaric acid and its derivatives exhibit broad clinical applications across various disease areas (Krefting *et al*., 2024). Mechanistically, they activate Nuclear factor erythroid 2-related factor 2 (Nrf2), reducing relapse rates in relapsing-remitting multiple sclerosis (RRMS), enhance the skin barrier function to alleviate the symptoms of atopic dermatitis and suppress Nuclear factor-kappa B (NF-κB)/Mitogen-activated protein kinase (MAPK) signaling to mitigate inflammatory cytokine release (Erler *et al*., 2024). Moreover, Fumaric acid modulates the balance of bone resorption and bone formation to relieve pain and reduces the expression of pro-inflammatory enzymes such as inducible nitric oxide synthase (iNOS) and cyclooxygenase-2 (COX-2) (Baldea *et al*., 2024). These findings demonstrate its potential in tumor-associated bone pain management. Fumarate derivatives activate Nrf2-dependent antioxidant pathways, upregulating Heme oxygenase-1 (HO-1), Glutathione S-transferases (GSTs) and NAD(P)H quinone oxidoreductase 1 (NQO1)1 (Patyk-Kaźmierczak *et al*., 2024). It not only enhances the antioxidant capacity of cells but also reduces the damage induced by oxidative stress to a certain extent. However, its specific targets in BCP and its function in opioid tolerance have not yet been clarified.

Mas-related G protein-coupled receptor member C (MrgC) is a sensory neuron receptor expressed in the dorsal root ganglia and spinal cord dorsal horn. As a class of receptors closely associated with sensory conduction and pain regulation, it has recently been demonstrated to be involved in the formation of various chronic pain states (Jiang *et al*., 2024). It can be activated by multiple endogenous ligands, such as neuropeptides and metabolites, thereby participating in the transmission and modulation of nociceptive information. MrgC can form heterodimers with MOR, negatively regulating the analgesic efficacy of morphine; its activation can also promote the release of mediators such as brain-derived neurotrophic factor (BDNF) from spinal microglia, further exacerbating pain sensitization (Yu *et al*., 2024). It has been reported that MrgC is also expressed in spinal microglia and its activation can induce the release of brain-derived neurotrophic factor, monocyte chemoattractant protein-1, etc. (Yu *et al*., 2024), promoting changes in neuronal plasticity. Additionally, the MrgC receptor further amplifies pain signals through Tumor necrosis

**Corresponding author:* e-mail: puhemao6@163.com

factor-alpha (TNF-α)/Interleukin-1 beta (IL-1β) regulation, playing a pivotal role in pain and drug tolerance. These findings make it an ideal target for exploring the cross-talk between pain, metabolism and immunity. However, little is known about the direct mechanistic link between MrgC-mediated fumarate analgesia and the regulation of opioid tolerance.

Based on the above background, this study hypothesizes that fumarate may modulate pain conduction and the progression of morphine tolerance in BCP states by regulating spinal MrgC receptors. To test this hypothesis, a BCP mouse model was established and a combination of behavioral, molecular biological and morphological methods was employed to systematically investigate the analgesic and anti-tolerance effects of fumarate, with a focus on elucidating the mediating role of MrgC in these processes. The aim is to provide new targets and theoretical foundations for overcoming opioid tolerance.

MATERIALS AND METHODS

Study design

This study employed a randomized, multi-dose level *in-vivo* animal experimental design. By establishing a mouse model of BCP, we systematically evaluated the analgesic effects of fumarate monotherapy and its combination with morphine, as well as their impact on morphine tolerance. The experimental groups were set as follows: Vehicle control group, fumarate monotherapy groups (25, 50, 100, 200, 400, 800 mg/kg), fumarate (100 mg/kg) + morphine (10 μg/kg) combination group, saline + morphine (10 μg/kg) control group and fumarate (100 mg/kg) + saline control group. All interventions were administered via an intrathecal catheter.

This study utilized a priori sample size calculation to ensure the strength of the evidence. Using G*Power 3.1 software, the calculation was based on an independent samples t-test model. The key parameters were set as follows: the primary outcome measure was the mechanical paw withdrawal threshold in the BCP model. Based on preliminary experimental data, a two-sided α of 0.05 and a power (1-β) of 0.90 were set and the effect size (d = 1.875) was estimated from literature and preliminary experiments. The calculation results indicated that a minimum of 8 animals per group was required. To account for potential attrition during the experiment, the sample size was increased by 20%, resulting in a final sample size of 10 animals per group.

Experimental materials

Male C57BL/6J mice (8 weeks old) were procured from the Department of Laboratory Animal Science, Peking University Health Science Center (License: SYXK [Beijing] 2021-0064). Animals were housed under specific pathogen-free (SPF) conditions with humidity (50–60%) and a 12-hour light/dark cycle. All mice had ad libitum access to food and water.

Main reagents and instruments: Fumaric acid (Chen Biotechnology Ltd.), morphine, fetal bovine serum (Omax Biotechnology Ltd.), antibiotic mixture (Merck, USA), Dulbecco's Modified Eagle Medium (DMEM) medium, Phosphate-buffered saline (PBS) (Hangzhou Meisen Cell Biotechnology Ltd.), Class II biosafety cabinet (Shanghai Bowen Instrument Ltd.), CO_2 incubator (Shanghai Bowen Instrument Ltd.), cell counter (Mettler Toledo), analgesiometer (Shanghai Yuyan Scientific Instrument Ltd., Model 2091), Lewis lung carcinoma (LLC) cells (Changsha Yideng Biology Co., Ltd), von Frey filament kit (Aesthesio), microsyringes (25μL/10μL, flat tip; Shanghai Gaoge), PE tubing (0.32×0.2 mm; Changsha Maiyue Biology Co., Ltd), bicinchoninic acid (BCA) protein assay kit (Thermo Fisher Scientific), rabbit anti-MrgC polyclonal antibody (Biorbyt, ORB101320) and MRGPRX1 rabbit polyclonal antibody (Biorbyt, ORB540455).

Methods

Cell culture and suspension preparation

Lewis lung carcinoma (LLC) cells (National Biomedical Experimental Cell Resource Bank, Peking Union Medical College) were thawed and cultured in DMEM supplemented with 10% Fetal bovine serum (FBS) and 1% antibiotics at 37°C/5% CO_2. Confluent cells were washed thrice with PBS, digested with 0.25% trypsin (3 min), neutralized with serum-containing DMEM, centrifuged (1000 rpm, 3 min) and resuspended in PBS. Cell density was adjusted to 4×10^8/mL using a cell counter.

Establishment of BCP mouse model

Under anesthesia with 3% isoflurane, mouse knee joints were exposed and 10μL LLC cell suspension (4×10^6/mL) was injected into the left femoral bone marrow cavity using a microsyringe; for the Naive group, only the same volume of PBS was injected and the needle was kept still for 2 minutes after injection (Chen *et al*., 2025). Mice exhibiting motor dysfunction, absence of hyperalgesia by day 14, or mortality were excluded.

Intrathecal catheterization

After anesthesia, the mice were placed in a prone position with their limbs fixed. The surgical site was localized at the L6 spinous process, identified as the intersection between the spinal midline and the interiliac crest line. A 1 cm longitudinal incision was made over the L5-L6 vertebral region. Using a 1 mL syringe needle angled 20–30° cephalad, the vertebral surface was punctured until dural penetration was confirmed by transient tail flick or hindlimb twitch. Following needle withdrawal, a 0.32 mm outer diameter PE catheter was advanced into the subarachnoid space along the rostral direction. A 5-0 mousse thread was used to ligate the paraspinal muscles and suture the incision to complete the surgical operation.

Randomization and blinding in experimental grouping and behavioral assessments

Eighty BCP mice were randomized into seven groups: Vehicle group (n=11), fumaric acid 25mg/kg group (n=12),

fumaric acid 50mg/kg group (n=12), fumaric acid 100mg/kg group (n=11), fumaric acid 200mg/kg group (n=11), fumaric acid 400mg/kg group (n=11) and fumaric acid 800mg/kg group (n=12). Forty additional model mice were divided into four groups (n=10/group) on day 14 post-modeling to induce morphine tolerance (7-day intrathecal regimen).

The analgesic effects of fumaric acid in BCP (BCP) mice were evaluated through a dose-optimization study comprising four experimental groups: the fumaric acid (100 mg/kg) + morphine (10 μg/kg) group received sequential intrathecal administration of fumaric acid followed by morphine after a 30-minute interval; the saline + morphine (10 μg/kg) group served as a control with intrathecal saline (5 μL) prior to morphine injection; the fumaric acid (100 mg/kg) + saline group was administered fumaric acid followed by saline after 30 minutes; and the vehicle group received intrathecal saline alone. Behavioral assessments were conducted at baseline (day 0) and at multiple post-inoculation time points (days 3, 7, 10, 14, 15, 16, 18 and 21), including quantification of spontaneous paw lifts, paw guarding duration, cold withdrawal latency and mechanical pain thresholds using Von Frey filaments. The 100 mg/kg fumaric acid dose was selected based on preliminary EC50 values (60–100 mg/kg) for further mechanistic analysis. Co-administration groups were designed to evaluate potential interactions between fumaric acid and morphine, while saline controls isolated compound-specific effects. The experimental timeline and protocol are illustrated in fig. 1.

All experimental animals were grouped using a random number table method after modeling to ensure consistent baseline levels across groups. During behavioral testing, the experimenters involved in the testing were not responsible for group allocation or drug administration and remained unaware of the group assignments. The scoring of pain behavior recordings was independently performed by another researcher who was also blinded to the experimental groups. During the data analysis phase, the analyst did not have access to group information until all statistical tests were completed, thereby ensuring blinded evaluation in both the behavioral testing and data analysis stages.

Drug preparation and administration

Mice were weighed prior to each administration to calculate individualized dosages. Fumaric acid powder was precisely weighed and dissolved in corn oil through 20-minute vortex mixing followed by volumetric adjustment. with subsequent volume adjustment and aliquot preparation. Prepared solutions were stored at 4°C. For subcutaneous administration, experimental groups received calculated drug doses, while control groups received equivalent volumes of PBS. In addition, the divided solution was accurately divided according to the dose of each mouse. Finally, the experimental group mice were administered drugs by gavage, while the control group mice received an equal volume of corn oil.

Pain behavior test

Spontaneous pain behavior test: Mice were placed in a plastic compartment with a transparent glass platform at the bottom and a 30-minute adaptation period was provided. Without external interference, spontaneous behaviors (left hindpaw lifting, licking and shaking) in the next 10 minutes were recorded.

Cold stimulation pain behavior test: Under quiet experimental conditions, the mice were first placed in a plastic compartment with a transparent glass platform at the bottom. Following a 30-minute environmental acclimation, a dry ice-containing device was positioned beneath the left hindpaw while ensuring that it was vertically aligned and in contact with the glass part directly below the left hindpaw of the mouse. The maximum contact time between dry ice and the glass platform was set to 20 seconds. When the mouse showed sudden foot lifting, licking, or shaking behavior under cold stimulation, these reactions were considered positive reactions. Each mouse was tested three times, with at least 10 minutes between each test. The time required for the mouse to have a positive reaction in each test was recorded and the average of the three measurement results was calculated. This average was used as the cold pain latency of the mouse.

Mechanical pain threshold test: Mice were placed on wire mesh platforms for 30-minute habituation. Von Frey fiber filaments (0.02g-2.0g) were applied to the center of the left hindpaw of the mouse for 5 s. Suddenly retracting their feet, licking their feet, or shaking their feet in response to the pressure applied by Von Frey fibers were considered positive reactions. Each specification of fiber required five measurements, with at least 10 minutes between each measurement. The minimal force eliciting three withdrawal responses across five trials was recorded as mechanical threshold. During the drug administration phase and withdrawal period, pain behavioral testing was uniformly scheduled within 3 h after the first administration of the day (Yang *et al*., 2024).

Thermal foot contraction incubation period (TWL) determination

Under controlled ambient temperature (20–25°C), mice were placed on a 55°C hot plate. TWL was defined as the latency from paw contact of the left hind foot of the mouse to nocifensive response (licking, lifting, or jumping). Baseline screening excluded animals showing responses <5 seconds or failing to respond within 30 s (Yang *et al*., 2024).

Hematoxylin-eosin staining (HE) staining

On the 21st day after Lewis lung cancer cell inoculation, left femurs were fixed in 4% paraformaldehyde (4°C, 24hrs) and decalcified over 3 weeks (weekly solution

replacement) during which the decalcification solution was changed once a week until the fine needle could easily penetrate the tissue. The bone samples that completed the decalcification process were first thoroughly washed with PBS, embedded in paraffin and continuously sectioned and the sections were successively cleared by xylene and dehydrated by ethanol gradient. After HE staining, the sections were sealed with neutral resin and the tissue structure was analyzed under an optical microscope (Yang *et al*., 2024).

Western blot detection

Lumbar spinal cord segments (L3-L5) were rapidly harvested under anesthesia (50mg/kg, i.p.) and homogenized in RIPA buffer containing PMSF (100:1). Lysates were centrifuged (13,000rpm, 10min, 4°C) and supernatants quantified via BCA assay with a BCA protein quantification kit (Thermo Fisher Scientific). Proteins were separated by SDS-PAGE, transferred to Polyvinylidene difluoride (PVDF) membranes and probed with primary anti-MrgC antibody (1:1000, Biorbyt ORB101320) overnight at 4°C. Then, the membrane was incubated with the Horseradish peroxidase (HRP)-conjugated secondary antibody at 37°C for 30 minutes and developed for colorimetric detection (Xie *et al*., 2025).

Immunohistochemical staining

The experimental mice were deeply anesthetized and physiological saline was injected intracardially to remove circulating blood. The lumbar spinal cord segments (L3 to L5) were fixed with 4% paraformaldehyde and blocked with 10% normal goat serum. The sections were incubated with primary anti-MrgC antibody (1:250, Biorbyt ORB101320) for 48hrs at 4°C, followed by secondary antibody (1:500, Biorbyt ORB540455) at 37°C for 30mins and HRP-conjugated secondary antibody (1:1000, Biorbyt ORB540455) (Chen *et al*., 2025).

Statistical analysis

The data are presented as mean ± standard deviation and were analyzed using SPSS 27.0 and GraphPad Prism 9.0. Prior to conducting parametric tests, the normality of all datasets was verified using the Shapiro-Wilk test. After confirming normal distribution, parametric statistical methods were applied for analysis. Behavioral time-series data were statistically analyzed using a two-way repeated-measures analysis of variance (ANOVA). When ANOVA indicated significant main effects or interaction effects, Tukey's post hoc test was utilized for pairwise comparisons between groups. The significance threshold was set at $P < 0.05$.

RESULTS

Successful construction of BCP model

To evaluate the interventional effects of fumarate in the BCP model, we first systematically analyzed its analgesic actions and its impact on morphine tolerance through pain behavioral indicators. The overall results demonstrated that fumarate not only alleviated BCP-related pain behaviors in a dose-dependent manner but also significantly delayed the development of analgesic tolerance induced by continuous morphine administration.

To evaluate the success of the construction of BCP mouse model, pain behavioral assessments from days 0-21 post-modeling were carried out. The experimental data showed that within days 7 to 14, mechanical withdrawal thresholds (MWT) and paw withdrawal latency (PWL) in the tumor-bearing left hindpaw of BCP mice were significantly reduced compared to Naive and PBS controls (Figs. 2A-B, P= 0.000). The number of spontaneous withdrawals and the protection time of the foot lifting increased ipsilaterally (Figs. 2C-2D, P=0.003), indicating that the left hindpaw had obvious hyperalgesia and lasted at least until the 21st day after modeling. The above results confirmed the effectiveness of the construction of BCP mouse model. Imaging analysis showed multiple osteolytic lesions with cortical thinning and discontinuity in BCP femurs, accompanied by periosteal inflammation and soft tissue swelling—findings absent in Vehicle controls (Fig. 2E). HE staining showed diffuse tumor infiltration and necrotic debris in BCP femurs, contrasting with intact marrow architecture in Vehicle mice (Fig. 2F).

Fumaric acid has significant analgesic and morphine tolerance induction effects on mice with BCP

The present study revealed that fumarate effectively alleviated BCP and delayed the development of morphine tolerance, with the 100 mg/kg dose, when combined with morphine, demonstrating the most significant effect. However, the improvement in cold pain sensitivity with the combination therapy was relatively limited. This may be attributed to differences in the neural pathways underlying distinct pain modalities. Cold pain sensation is primarily mediated by C-fibers, whereas the synergistic effect of fumarate and morphine may predominantly target Aδ fiber-mediated mechanical and thermal pain pathways.

The fumaric acid (100 mg/kg) + morphine (10 μg/kg) cohort exhibited superior MWT from days 0–13 compared to other groups, though efficacy declined over time. Similarly, the TWL of this group was significantly higher than that of other groups at day 13, although the TWL showed a shortening trend overall (Figs. 3A-3B). During days 2-7, this combination group maintained significantly higher MWT than morphine-alone (Vehicle + morphine) and fumaric acid-alone (fumaric acid + Vehicle) groups (Fig. 3C). Meanwhile, the TWL of the fumaric acid 100 mg/kg + morphine 10 μg/kg group was significantly higher than that of the other groups after the 1st day and the TWL gradually shortened over time (Fig. 3D).

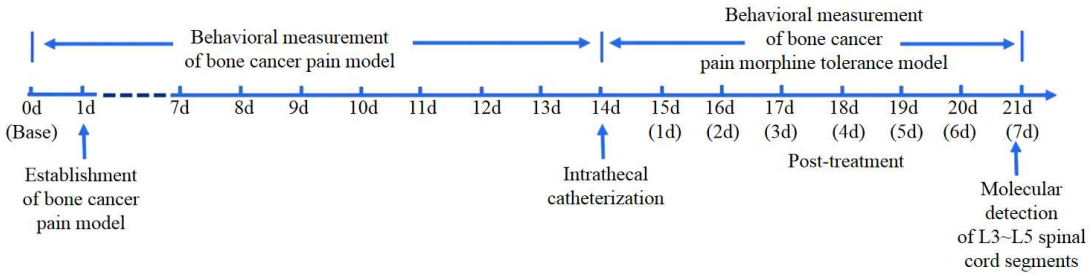

Fig. 1: Experimental intervention flow chart. The schematic diagram illustrates the key steps of the study, including the establishment of the bone cancer pain (BCP) model on day 0, initiation of intrathecal drug administration on day 14, behavioral testing schedule (days 3, 7, 10, 14, 15, 16, 18 and 21) and terminal tissue collection on day 21.

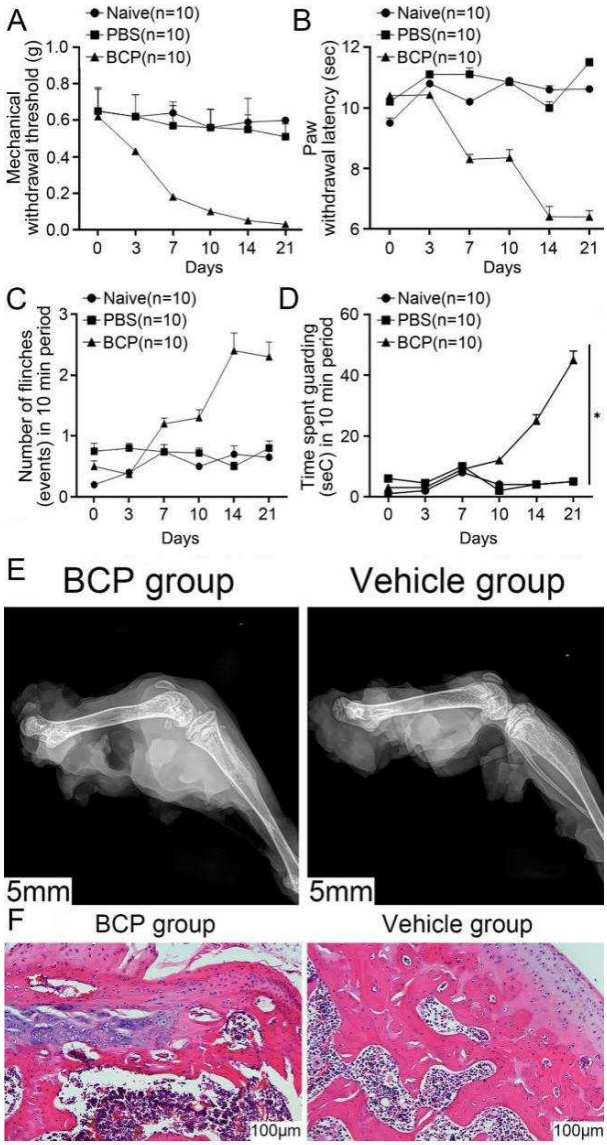

Fig. 2: The BCP model was successfully constructed. (A) Threshold of mechanical stimulation withdrawal reflex of the left (tumor-bearing) hindpaw of mice; (B) Latency of withdrawal to cold pain stimulation; (C) Number of spontaneous withdrawals of the ipsilateral hindpaw; (D). Lifting protection time; (E) Imaging results of the left femur of BCP mice inoculated with Lewis lung cancer cells for 21 days; (F) HE staining results of the left femur of mice 21 days after cell inoculation (HEx400)

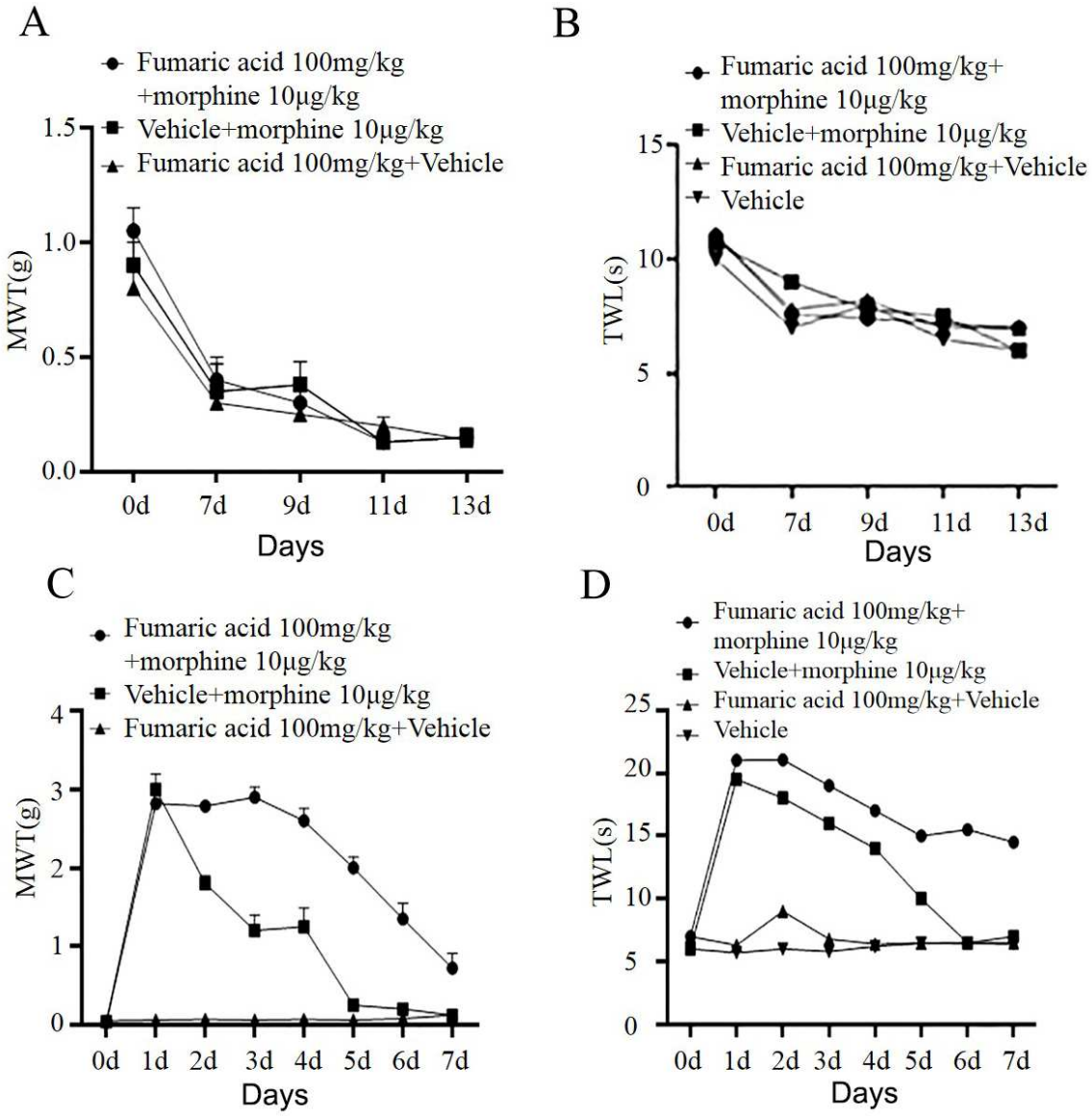

Fig. 3: Fumaric acid has significant analgesic and morphine tolerance-inducing effects on mice with bone cancer pain. (A) 0-13d mechanical paw withdrawal threshold MWT; (B) 0-13d thermal paw withdrawal latency TWL; (C) 0-7d mechanical paw withdrawal threshold MWT; (D) 0-7d thermal paw withdrawal latency TWL

Post-withdrawal analgesic effect of fumaric acid on BCP in mice and determination of EC50

This study confirmed that fumarate maintained stable analgesic effects even after drug withdrawal, with its analgesic activity demonstrating a dose-dependent profile within the effective dose range of 60-100 mg/kg. Notably, the 800 mg/kg dose group exhibited reduced analgesic efficacy accompanied by toxic reactions, indicating that exceeding the optimal dosage range may lead to adverse effects.

Comparative analysis revealed that BCP model mice administered fumaric acid at ≥50 mg/kg exhibited significant increases in MWT and PWL from the third day after administration (Figs. 4A-4B, P=0.007). Notably, spontaneous paw lifts and protective lifting duration in the ipsilateral hindpaw showed marked reduction from day 7 in treatment groups receiving ≥50 mg/kg fumaric acid (Figs. 4C-4D, P=0.038). This shows that fumaric acid has a significant analgesic effect on BCP mice. Further study of the effect of different doses of fumaric acid on the MWT (Fig. 4E, P=0.000) and TWL (Fig. 4F, P=0.005) of mice from 0 to 24 days was carried out. Dose-response analysis demonstrated maximal efficacy at 100 mg/kg for both MWT (Fig. 4E) and TWL (Fig. 4F) across 0-24 days. While the 800 mg/kg dose exhibited reduced analgesic efficacy accompanied by signs of drug toxicity, post-cessation evaluations revealed stable analgesic maintenance for 24 hours (Figs. 4A-D).

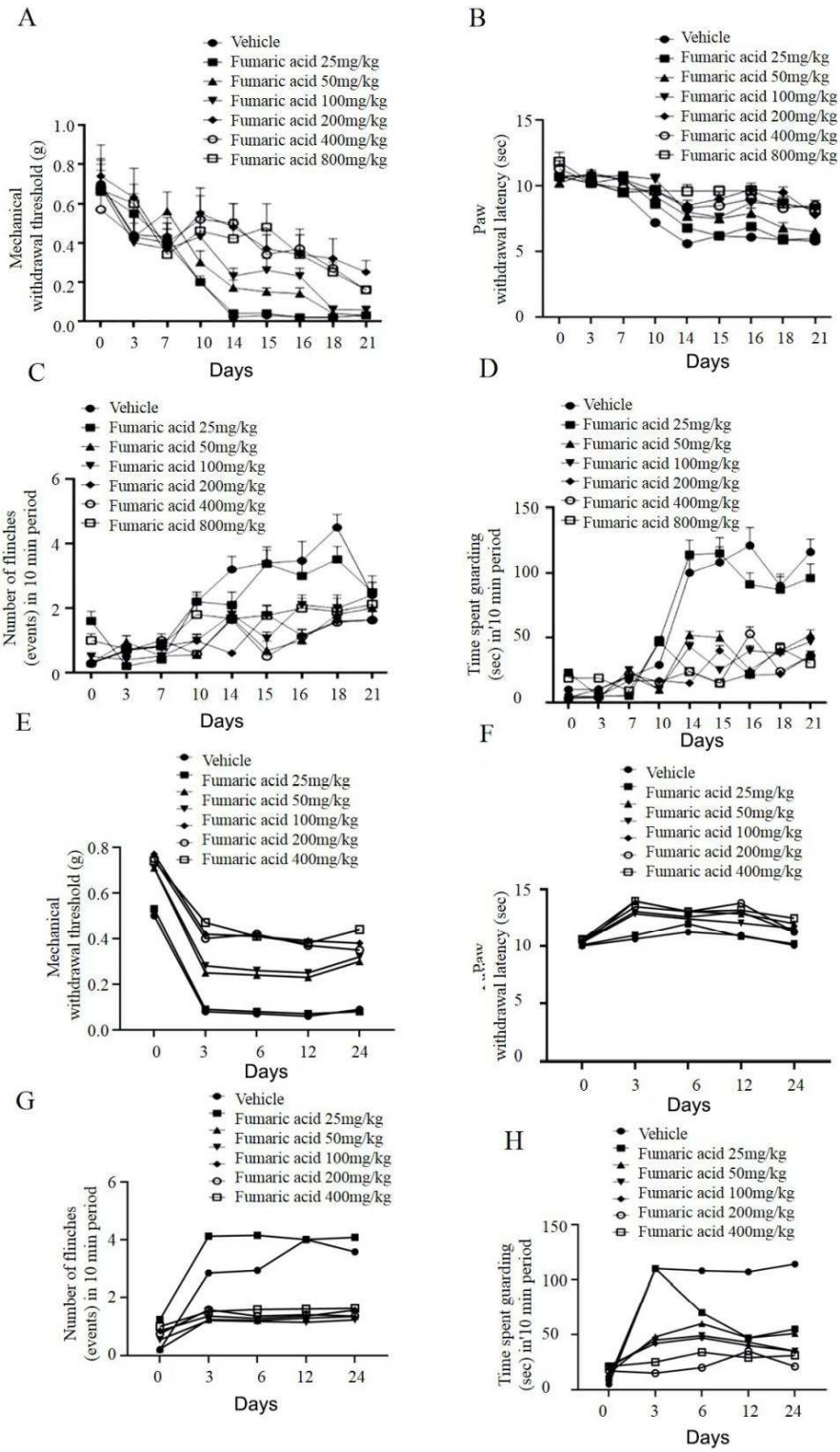

Fig. 4: Post-drug analgesic effect of fumaric acid on BCP mice and determination of EC50. (A-D) Time course of pain behaviors from day 0 to 21 after treatment with different doses of fumarate (25-800 mg/kg): (A) Mechanical withdrawal threshold (MWT); (B) Thermal withdrawal latency (TWL); (C) Number of spontaneous paw lifts;(D) Paw elevation duration. (E-H) Dose-response analysis of fumarate from day 0 to 24: (E) Mechanical withdrawal threshold (MWT);(F) Thermal withdrawal latency (TWL); (G) Number of spontaneous paw lifts;(H) Mechanical withdrawal threshold (MWT) at 48 hours after drug withdrawal, used for EC_{50} calculation. The effective concentration range (60-100 mg/kg) and EC_{50} values for mechanical analgesia (69.18 mg/kg) and cold analgesia (99.78 mg/kg) are indicated.

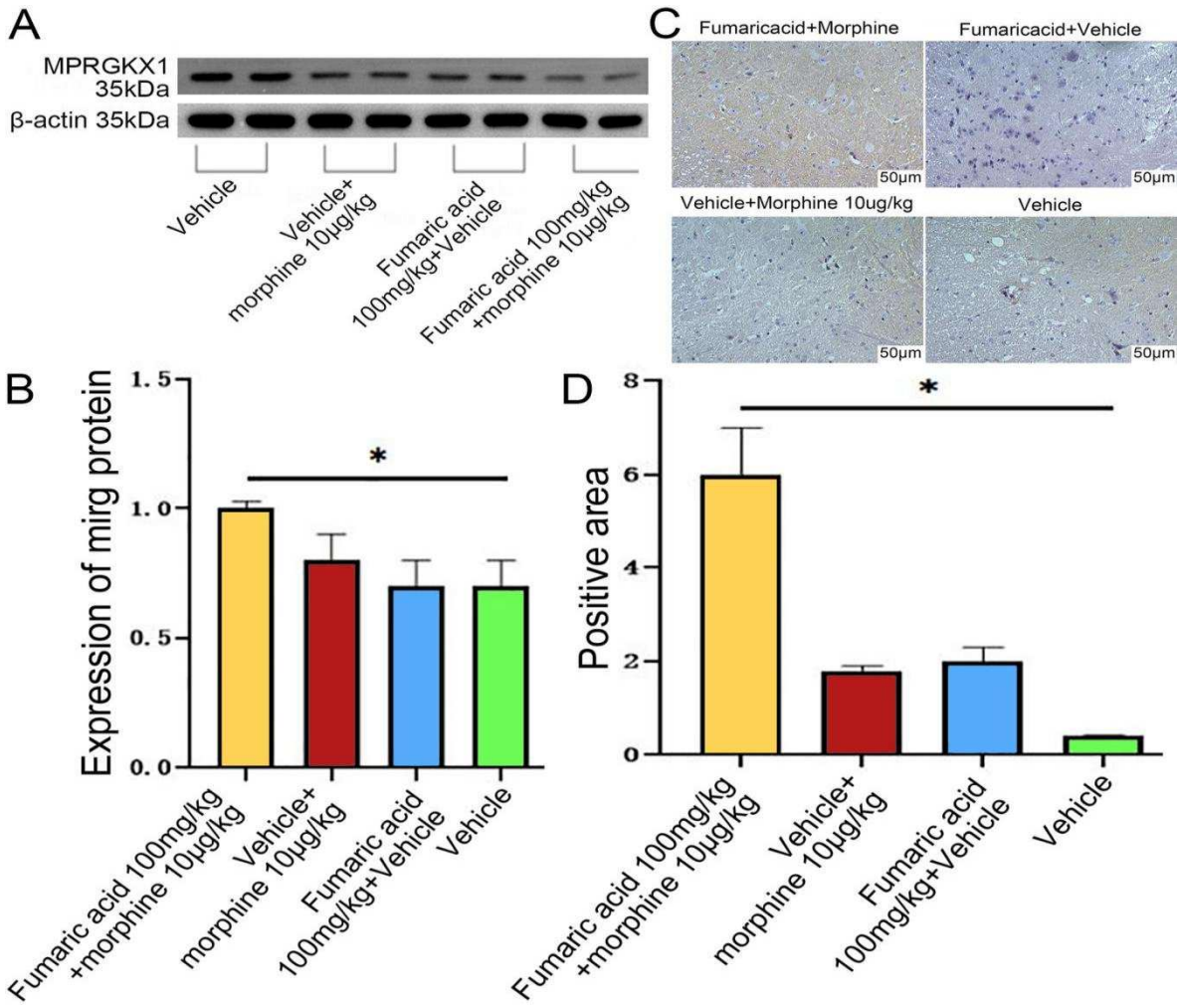

Fig. 5: Fumaric acid analgesic effect on BCP mice is achieved through activation of spinal MrgC receptor. (A) Western Blot detection of protein expression; (B) Quantitative analysis of protein level results; (C) Representative images of immunohistochemical detection of MrgC receptor protein expression in the spinal cord of each group of mice, with arrows pointing to positive products; (D) Positive area.

At 48 hours after drug withdrawal, the dose-effect curve drawn by combining the MWT and PWL of the ipsilateral hindpaw found that the EC50 of fumaric acid for mechanical and cold analgesia was 69.18 mg/kg and 99.78 mg/kg, respectively, with an effective concentration range of 60-100 mg/kg. All fumaric acid treatment groups showed significant improvements in spontaneous paw lift frequency and duration (Figs. 4G-4H).

Analgesia of fumaric acid on BCP mice is achieved through activation of spinal MrgC receptors

The primary mechanistic finding of this study is that the analgesic effect of fumarate is closely associated with the modulation of spinal MrgC receptors.

Western blot was conducted to detect the expression of MrgC protein under different treatment conditions. The quantitative analysis revealed significant MrgC protein downregulation in the fumaric acid 100 mg/kg + Vehicle group compared to morphine-containing treatment groups (10 μg/kg) (Figs. 5A-5B, P=0.000). These results suggest that fumaric acid and morphine alone or in combination can decrease expression of MrgC protein and the effect is more significant when used in combination (Figs. 5A-5B). Immunohistochemistry consistently indicated that the Vehicle group had more positive staining areas and a higher expression level of MrgC protein, whereas combination of fumaric acid and morphine reduced positive staining areas on tissue sections and the expression level of MrgC protein; compared with the use of Vehicle alone, the fumaric acid + Vehicle group also had fewer positive staining areas and inhibited MrgC protein expression (Fig. 5C-5D).

DISCUSSION

MCP-1 and its receptor CCR2 expression in the spinal cord of morphine-tolerant rats with BCP are significantly upregulated, activating microglia, promoting the release of

inflammatory factors and aggravating pain sensitization and morphine tolerance (Xie *et al*., 2024). For patients with BCP, long-term morphine use leads to hypertrophy of spinal astrocytes (Zhang *et al*., 2024) and decreased expression of glutamate reuptake transporters, which will increase extracellular glutamate concentrations, enhance central sensitization and produce tolerance (Li *et al*., 2024). Some studies have used β-elemene to inhibit the expression of NMDA receptor subunit NR2B to improve morphine tolerance (Lipina *et al*., 2024). In this study, within 7 to 14 days after LLC cell inoculation, the MWT and PWL of the tumor-side hindpaws of mice in the BCP group were significantly lower than those in the Naive group and the PBS group, indicating obvious hyperalgesia in the BCP mice. In addition, the number of spontaneous foot retractions and the length of foot protection time on the ipsilateral hindpaw increased, further confirming the persistent hyperalgesia of the left hindpaw. The results suggest that the destructive effect of tumor cells on bone structure presents multiple perforated osteolytic lesions and thinning of the bone cortex. This pathological change is mainly responsible for tumor-related bone pain. The invasion and proliferation of tumor cells directly destroy bone tissue, induce changes in the local microenvironment and promote inflammatory response and pain. (Zhang *et al*., 2024) pointed out that these structural alterations, driven by metastatic tumor cell secretion of IL-8, VEGF and MMPs lead to thinning of the bone cortex and osteolytic lesions and then cause severe bone pain. In subsequent experiments, the Vehicle group served as a control to verify the effectiveness and specificity of the experimental operation and to exclude the influence of nonspecific factors.

Chronic morphine exposure induces sustained μ-opioid receptor (MOR) activation, triggering receptor phosphorylation and β-arrestin coupling. This process is exacerbated by GSNOR downregulation-mediated S-nitrosylation of PKCα (Zhang *et al*., 2024), which impairs receptor desensitization and reduces endocytosis. In addition, studies have found that morphine-induced HMGB1 release from neurons activates microglial TLR4/NF-κB signaling (Shao *et al*., 2024) upregulating proinflammatory factors such as IL-1β and accelerating morphine tolerance. In this study, the MWT and TWL of the F100+M group were significantly higher than those of the other groups within 0-7 days. This suggests that fumaric acid 100 mg/kg combined with morphine might strengthen the analgesic effect in the short term, inhibiting peripheral and central sensitization through synergistic effects. Furthermore, the enhanced effect versus F100 alone indicates morphine remains the primary analgesic component, with fumaric acid potentiating its activity through anti-inflammatory mechanisms and receptor signaling modulation. Fumaric acid can reduce central sensitization by inhibiting the TLR4/NF-κB pathway of spinal microglia, reducing the release of proinflammatory IL-6 and TNF-α factors (Xaviera *et al*., 2024). However, the limited cold pain sensitivity improvement in combination therapy suggests fumaric acid-morphine synergy primarily targets Aδ/C fiber-mediated mechanical and thermal pain pathways. In the study, fumaric acid (≥50 mg/kg) significantly improved MWT and TWL, suggesting that its rapid inhibitory effect on peripheral pain sensitization is mainly due to its inhibition of spinal microglia OX-42 markers, astrocytes (GFAP markers) activation and reduced release of pain mediators such as ATP and BDNF (Chen *et al*., 2022). The regulatory effect of fumaric acid on central sensitization, hyperexcitability of spinal dorsal horn neurons and neuropathic pain gradually increased, which may be related to the inhibition of glial cell activation or the regulation of NMDA receptor function (Zhao *et al*., 2025). The 100 mg/kg group continued to show the highest MWT and TWL within 24 hours, suggesting that its EC50 may be close to this dose range, while 800 mg/kg toxicity underscores its direct pain pathway engagement rather than placebo effects and demonstrated diminished analgesic efficacy accompanied by signs of toxicity, indicating the existence of a well-defined therapeutic window. This finding provides crucial guidance for clinical dosage selection. Long-term morphine exposure causes continuous activation of MOR, leading to its phosphorylation and binding to β-arrestin, causing receptor desensitization and reduced endocytosis (Underwood *et al*., 2024). This process involves S-nitrosylation modification of PKCα, inhibition PKC kinase activity and suppression of receptor resensitization as morphine reduces cAMP by inhibiting adenylate cyclase (AC) (Huang *et al*., 2024). And long-term use will lead to compensatory activation of AC. Normally, ATP released after activation of spinal microglia enhances neuronal excitability through P2X4 receptors. Cancer pain is often accompanied by the release of inflammatory factors and neuropathic changes. MrgC receptor activation exerts dual inhibitory effects on key pain pathways through TLR4/NF-κB signaling suppression and NMDA receptor activity modulation (Dash *et al*., 2024). This dual mechanism reduces NMDA receptor-mediated calcium influx, subsequently diminishing PKC activation and nitric oxide synthase (NOS) expression (Huang *et al*., 2021) thereby disrupting the critical "calcium-kinase-oxidative stress" cascade underlying hyperalgesia development. Concurrently, MrgC activation modulates voltage-gated sodium channel (Nav1.8) activity in dorsal root ganglion neurons, decreasing action potential firing frequency (Dash *et al*., 2024) to alleviate pain caused by bone metastasis and tumor compression. Genetic evidence from inflammatory pain models demonstrates that MrgC-knockout mice exhibit prolonged hyperalgesia with 2-3 fold elevations in spinal IL-1β and TNF-α concentrations compared to wild-type controls (Jiang *et al*., 2024). Although current research focuses on inflammatory pain, similar neuroinflammation and central sensitization mechanisms in cancer pain treatment suggest that MrgC receptors may

become new targets. In this study, fumaric acid-morphine combination therapy produces additive MrgC suppression ($p<0.001$ vs monotherapy), as fumaric acid or morphine alone can reduce MrgC protein expression. As an intermediate product in the tricarboxylic acid cycle, fumaric acid can directly affect the intracellular energy state and metabolite concentration, thereby regulating gene expression and the synthesis of various proteins, including the MrgC protein. This not only provides new insights into pain management but also opens up a new direction for a deeper understanding of the role of MrgC protein in pathophysiological processes.

This study provides a detailed elucidation of fumarate's role in delaying morphine tolerance within a BCP model and, for the first time, reveals the critical mediating function of spinal MrgC receptors in this process, thereby offering a novel potential target and strategy for overcoming opioid tolerance. A comprehensive suite of *in-vivo* behavioral assessments was employed to validate the analgesic and tolerance-modulating effects of fumarate across multiple dimensions. Furthermore, a multi-dose gradient design was implemented, which clearly delineated the dose-response relationship of fumarate and furnished experimental evidence for its effective dosage range. Additionally, the study incorporated molecular biology techniques to preliminarily explore the underlying downstream mechanisms at the protein expression level, thereby strengthening the reliability of the findings.

However, the conclusions of this study primarily rely on animal behavioral data and correlative protein expression analyses. It did not fully elucidate the specific upstream signaling pathways through which fumarate modulates MrgC expression. The absence of MrgC gene knockout models or selective antagonists means that more direct causal evidence supporting the necessity of MrgC in this process is lacking. Moreover, the experimental observation period was relatively short, precluding an evaluation of the long-term efficacy and safety of fumarate application. These aspects represent important directions for future in-depth investigation.

CONCLUSION

In summary, fumarate alleviates BCP and delays the development of morphine tolerance by downregulating spinal MrgC receptor expression. Furthermore, fumarate exerts synergistic effects through multi-target mechanisms, including the inhibition of glial cell activation and modulation of NMDA receptor function. Future studies should focus on long-term administration experiments to elucidate the upstream signaling pathways through which fumarate regulates MrgC expression and to identify its direct molecular targets. A comprehensive evaluation of fumarate's safety profile and long-term efficacy is also warranted. Additionally, employing MrgC gene-knockout models or specific antagonists could verify the necessity of MrgC for mediating the effects of fumarate. It is also worthwhile to explore combination therapies of fumarate with other analgesic agents, which may yield enhanced therapeutic outcomes with reduced side effects.

This study not only reveals the critical role of the MrgC receptor in opioid tolerance but also provides a theoretical foundation for developing novel analgesic drugs based on the fumarate structure.

Acknowledgments
None.

Authors' contributions
Jidong Lv: Proposed the research hypothesis and designed the overall experimental scheme. Participated in the optimization of the experimental design and the application for ethical approval and drafted the initial manuscript; Sijie Liu: Responsible for the culture of Lewis lung carcinoma cells and the establishment of the BCP mouse model. Performed intrathecal catheter implantation surgeries and provided postoperative animal care; Minghao Tang: Conducted behavioral tests for mechanical, cold and thermal pain, recorded and performed preliminary analysis of spontaneous pain behaviors. All behavioral scoring was independently carried out under blinded conditions; Jing Zhao: Responsible for Western blot experiments and immunohistochemical staining. Participated in sample processing, protein quantification and image acquisition; Lulu Zhang: Performed data processing and statistical analysis using GraphPad Prism 9.0, assisted in EC_{50} calculation and graph preparation. All authors participated in reviewing and revising the manuscript and approved the final version for submission.

Funding
There was no funding.

Data availability statement
The datasets generated during and/or analysed during the current study are available from the corresponding author on reasonable request.

Ethical approval
This study was approved by the ethics committee of Jiashan First People's Hospital. Experimental protocols adhered to International Association for the Study of Pain guidelines and were approved by the Institutional Animal Care and Use Committee of Peking University Health Science Center (Ethics Approval: BCJB0019). Efforts were made to minimize animal discomfort and reduce sample sizes. This study was performed in adherence with

the ARRIVE guidelines. See supplementary file for the ARRIVE checklist.

Conflict of interest

There are no conflicts to declare.

Supplementary data

https://www.pjps.pk/uploads/2026/06/SUP1780569460.pdf

REFERENCES

Ahmadi S, Majidi M, Koraei M and Vasef S (2024). The inflammation/NF-κB and BDNF/TrkB/CREB pathways in the cerebellum are implicated in the changes in spatial working memory after both morphine dependence and withdrawal in rat. *Mol Neurobiol*., **61**(9): 6721–6733.

Baldea I, Moldovan R, Nagy AL, Bolfa P, Decea R, Miclaus MO, Lung I, Gherman AMR, Sevastre-Berghian A, Martin FA, Kacso I and Răzniceanu V (2024). Ketoconazole-Fumaric acid pharmaceutical cocrystal: From formulation design for bioavailability improvement to biocompatibility testing and antifungal efficacy evaluation. *Int J Mol Sci*., **25**(24): 13346.

Chen X, Zeng Y, Wang Z, Zhu J, Liu F, Zhu M, Zheng J, Chen Q, Zhai D, Chen Y, Niu J, Xue Z, Sun G, Li F, Pan Z (2025). NFAT1 signaling contributes to bone cancer pain by regulating IL-18 expression in spinal microglia. *CNS Neurosci Ther*., **31**(2):e70222.

Chen Y, Luo Z, Sun Y, Li F, Han Z, Qi B, Lin J, Lin WW, Yao M, Kang X, Huang J, Sun, C, Ying C, Guo C, Xu Y, Chen J and Chen S (2022). Exercise improves choroid plexus epithelial cells metabolism to prevent glial cell-associated neurodegeneration. *Front Pharmacol*., **13**: 1010785.

Dash PP, Mohanty P, Behura R, Behera S, Naik S, Mishra M, Sahoo H, Barick AK, Mohapatra P, Sahoo SK and Jali BR (2024). Rapid colorimetric and fluorometric discrimination of maleic acid vs. fumaric acid and detection of maleic acid in food additives. *J Fluoresc*., **34**(3): 1015–1024.

Erler K, Krafczyk N, Steinbrenner H and Klotz LO (2024). Selective activation of cellular stress response pathways by fumaric acid esters. *FEBS Open Bio*., **14**(8): 1230–1246.

Huang Q, Ford NC, Gao X, Chen Z, Guo R, Raja SN, Guan Y and He S (2021). Ubiquitin-mediated receptor degradation contributes to development of tolerance to MrgC agonist-induced pain inhibition in neuropathic rats. *Pain*., **162**(4): 1082–1094.

Khalaf MM, Mahmoud HM, Kandeil MA, Mahmoud HA and Salama AA (2024). Fumaric acid protects rats from ciprofloxacin-provoked depression through modulating TLR4, Nrf-2 and p190-rho GTP. *Drug Chem Toxicol*., **47**(6): 897–908.

Krefting F, Hölsken S, Schedlowski M and Sondermann W (2024). Discontinuation of fumaric acid esters is affected by depressive symptomatology: A retrospective analysis. *Acta Derm Venereol*., **104**: 12326.

Jiang JP, Zhang K, Hu FJ and Hong YG (2024). Mas-related gene C (MrgC) receptor activation induced inhibition of neurochemical alterations in the spinal dorsal horn and dorsal root ganglia in a rat model of bone cancer pain. *Sheng Li Xue Bao*., **76**(6): 953–969.

Li S, Tang S, Dai L, Jian Z and Li X (2024). Emodin relieves morphine-stimulated BV2 microglial activation and inflammation through the TLR4/NF-κB/NLRP3 pathway. *Neuroreport*., **35**(8): 518–528.

Lipina TV, Giang H, Thacker JS, Wetsel WC, Caron MG, Beaulieu JM, Salahpour A and Ramsey AJ (2024). Combination of haloperidol with UNC9994, β-arrestin-biased analog of aripiprazole, ameliorates schizophrenia-related phenotypes induced by NMDAR deficit in mice. *Int J Neuropsychopharmacol*., **27**(12): pyae060.

Ni C, Chen L, Hua B, Han Z, Xu L, Zhou Q, Yao M and Ni H (2024). Epigenetic mechanisms of bone cancer pain. *Neuropharmacology*., **261**: 110164.

Patyk-Kaźmierczak E and Kaźmierczak M (2024). Metal-free negative linear compressibility (NLC) material - the cocrystal of 1, 2-bis(4-pyridyl)ethane and fumaric acid. *Chem Commun (Camb)*., **60**(75): 10310–10313.

Shao X, Xie L, Zhai J and Ge M (2024). Postoperative analgesia with morphine promoting microglial activation and neuroinflammation induced by surgery aggravates perioperative neurocognitive dysfunction in aged mice. *IBRO Neurosci Rep*., **18**: 39–49.

Underwood O, Fritzwanker S, Glenn J, Blum NK, Batista-Gondin A, Drube J, Hoffmann C, Briddon SJ, Schulz S and Canals M (2024). Key phosphorylation sites for robust β-arrestin2 binding at the MOR revisited. *Commun Biol*., **7**(1): 933.

Xaviera A, Saleem A, Akhtar MF, Alshammari A and Albekairi NA (2024). Fumaric acid per se and in combination with methotrexate arrests inflammation via moderating inflammatory and oxidative stress biomarkers in arthritic rats. *Immunopharmacol Immunotoxicol*., **46**(6): 793–804.

Xie M, Li D, Zeng H, Huang Y, Xu R, Wang Z, Yu J, Sun Y (2025). BAM8-22 targets spinal MrgC receptors to modulate UPRmt activity in the mechanism of bone cancer pain. *Front Pharmacol*., **16**: 1575733.

Xie F, Kitagawa Y, Ogata H, Yasuhara S, You Z and Jeevendra Martyn JA (2024). Morphine induces inflammatory responses via both TLR4 and cGAS-STING signaling pathways. *Cytokine*., **183**: 156737.

Yang L, Li M, Liu Y, Bai Y, Yin T, Chen Y, Jiang J, Liu S (2024). MOTS-c is an effective target for treating cancer-induced bone pain through the induction of AMPK-mediated mitochondrial biogenesis. *Acta Biochim Biophys Sin (Shanghai)*., **56**(9): 1323-1339.

Yu J, Li D, Xie M, Xie J, Wang Z, Gu X, Ma Z and Sun Y (2024). Complex topology of ubiquitin chains mediates lysosomal degradation of MrgC proteins. *Cell Biochem Biophys*., **82**(2): 641–645.

Zhang F, Dong Y, Chen F, Niu M, Liu Z and Wang C (2024). Cinobufotalin capsule combined with zoledronic acid in the treatment of pain symptoms and clinical efficacy in prostate cancer patients with bone metastases: A retrospective study. *Arch Esp Urol*., **77**(3): 242–248.

Zhang H, Jiang J, Chen X, Zhu F, Fu F, Chen A, Fu L and Mao D (2024). Liu-Shen-Wan inhibits PI3K/Akt and TRPV1 signaling alleviating bone cancer pain in rats. *Cancer Biol Ther*., **25**(1): 2432098.

Zhao J, Zhang Y, Lv S, Wang F, Shan T, Wang J, Liu Z, Zhang L, Cui H and Tian J (2025). Mechanism of formononetin in improving energy metabolism and alleviating neuronal injury in CIRI based on nontargeted metabolomics research. *J Cell Mol Med*., **29**(4): e70340.